

Competition between different order parameters in a quasi-one-dimensional superconductor

A. V. Rozhkov

Institute for Theoretical and Applied Electrodynamics, RAS, ul. Izhorskaya 13/19, Moscow 125412, Russian Federation

(Received 6 October 2008; published 2 June 2009; corrected 8 June 2009)

We show that, under rather general assumptions, the phase diagram of a quasi-one-dimensional repulsive Fermi system consists of two ordered phases: the density wave, spin or charge, and the superconductivity. It is demonstrated that the symmetry of the superconducting order parameter is a nonuniversal property sensitive to microscopic details of the model. Three potentially stable superconducting states are identified: they are triplet f -wave, singlet $d_{x^2-y^2}$ -wave, and d_{xy} -wave. The presence of multiple competing superconducting states implies that for a real material this symmetry is difficult to predict theoretically and hard to probe experimentally since artifacts of theoretical approximations or variations in experimental conditions could tip the balance between the superconducting phases.

DOI: [10.1103/PhysRevB.79.224501](https://doi.org/10.1103/PhysRevB.79.224501)

PACS number(s): 74.20.Mn, 74.20.Rp, 74.70.Kn

I. INTRODUCTION

Many theorists hold that the superconductivity in quasi-one-dimensional (Q1D) materials may be explained with the help nonphonon many-body mechanism.¹⁻¹⁷ Yet, there is substantial disagreement about the details of such mechanism. Moreover, different theories predict different order-parameter symmetries: p , $d_{x^2-y^2}$, f , or d_{xy} wave.⁸⁻¹¹ The experimental findings¹⁸⁻²⁵ have been unable to resolve these controversies.

In this paper we explain why establishing the symmetry of the order parameter is such a hard task. It will be demonstrated that within the framework of the nonphonon mechanism there are three metastable superconducting states, $d_{x^2-y^2}$, f , and d_{xy} wave, which compete to become the ground state. This circumstance has an important implication for both theory and experiment: to find the ground-state symmetry one has to resolve small energy differences between the contesting states. Thus, an approximate theoretical scheme might calculate these differences completely wrong; a slight variation in the model may cause a phase transition. An experimentalist has to keep in mind that, despite the obvious similarities between various families of the Q1D superconducting materials in chemistry and structure and despite “universality” of their phase diagram,²⁵ the superconducting order does not have to be identical in all these metals. Moreover, even an individual sample may experience phase transitions between different types of superconductivity as the pressure or magnetic-field change (e.g., Ref. 24). This suggests that experimental detection of the order-parameter symmetry should be done for a specific material rather than a class of materials; a reliable theoretical prediction of this symmetry is nearly impossible.

Let us briefly outline main ideas of the discussion. Due to the presence of nonperturbative many-body effects, the Q1D metal cannot be treated by the usual mean-field theory. Thus, to circumvent this difficulty, we derive the low-energy effective Hamiltonian. Unlike the original microscopic model, the anisotropy of the effective model is low, and it may be studied with the help of the mean-field approximation. Application of mean-field theory to the effective model^{1,2} allows us to find the phase diagram of the Q1D metal. At good nesting

the system freezes into a spin-density (SDW) or charge-density wave (CDW). The antineesting destroys the density-wave phase and makes superconductivity possible. In superconducting phase we find three order parameters, which may be stable in our model.

The paper is organized as follows. The Q1D model and its effective low-energy description are presented in Sec. II. The phase diagram is obtained in Sec. III. Section IV is reserved for discussion of the results.

II. Q1D MODEL AND ITS EFFECTIVE HAMILTONIAN

A. Bare Hamiltonian

The model we study is well known. The system consists of one-dimensional (1D) chains, which are arranged into a square array to form a three-dimensional (3D) system. Its Hamiltonian has the form

$$H = \sum_i H_i^{\text{1D}} + \sum_{ij} H_{ij}^{\text{hop}} + H_{ij}^{\text{pp}}, \quad (1)$$

where H_i^{1D} is the Hamiltonian of an individual 1D chain i ,

$$H_i^{\text{1D}} = H_i^{\text{kin}} + H_i^{\text{pp}}, \quad (2)$$

$$H_i^{\text{kin}} = -iv_F \sum_{p\sigma} p \int dx: \psi_{p\sigma i}^\dagger (\nabla \psi_{p\sigma i}):, \quad (3)$$

$$H_i^{\text{pp}} = \int dx [-J_{2k_F} \mathbf{S}_{2k_F i} \cdot \mathbf{S}_{-2k_F i} - g_{2k_F} \rho_{2k_F i} \rho_{-2k_F i} + g_4 (\rho_{L\uparrow i} \rho_{L\downarrow i} + \rho_{R\uparrow i} \rho_{R\downarrow i})], \quad (4)$$

$$\rho_{p\sigma} = : \psi_{p\sigma}^\dagger \psi_{p\sigma} :, \quad (5)$$

$$\rho_{2k_F} = \sum_{\sigma} \psi_{R\sigma}^\dagger \psi_{L\sigma}, \quad \rho_{-2k_F} = \rho_{2k_F}^\dagger, \quad (6)$$

$$\mathbf{S}_{2k_F} = \sum_{\sigma\sigma'} \vec{\tau}_{\sigma\sigma'} \psi_{R\sigma}^\dagger \psi_{L\sigma'}, \quad \mathbf{S}_{-2k_F} = \mathbf{S}_{2k_F}^\dagger. \quad (7)$$

Here index $p = \pm 1$ labels different chiralities of 1D electrons, right movers $\psi_{R\sigma}$ ($p=1$) and left movers $\psi_{L\sigma}$ ($p=-1$).

Vector $\vec{\tau}$ is composed of three Pauli matrices. The coupling constants $g_{4,2k_F}$ and J_{2k_F} are positive, which corresponds to repulsion between electrons. The model's microscopic cutoff is denoted by Λ .

We expressed our Hamiltonian H_i^{pp} in a somewhat unusual form. In a more traditional notation this operator looks as such,

$$H_i^{pp} = \int dx \left[g_1 \rho_{2k_F i} \rho_{-2k_F i} + g_2 \sum_{\sigma\sigma'} \rho_{L\sigma i} \rho_{R\sigma' i} + g_4 (\rho_{L\uparrow i} \rho_{L\downarrow i} + \rho_{R\uparrow i} \rho_{R\downarrow i}) \right], \quad (8)$$

$$g_{2k_F} = \frac{g_2}{2} - g_1, \quad (9)$$

$$J_{2k_F} = \frac{g_2}{2}. \quad (10)$$

Both forms are absolutely equivalent. Equation (4) suits us more for it explicitly shows the couplings of the density waves.

Closely located chains are coupled by single-electron hopping H_{ij}^{hop} and electron-electron interaction H_{ij}^{pp} ,

$$H_{ij}^{\text{hop}} = -t(i-j) \sum_{p\sigma} \int dx (\psi_{p\sigma i}^\dagger \psi_{p\sigma j} + \text{H.c.}), \quad (11)$$

$$H_{ij}^{pp} = \int dx [g_0^\perp (i-j) \rho_i \rho_j + g_{2k_F}^\perp (i-j) (\rho_{2k_F i} \rho_{-2k_F j} + \text{H.c.})], \quad (12)$$

$$\rho = \sum_{p\sigma} \rho_{p\sigma}. \quad (13)$$

We assume that our microscopic model is characterized by the following hierarchy of material constants. The anisotropy ratio is small,

$$r = t/v_F \Lambda \ll 1. \quad (14)$$

In addition, the $2k_F$ coupling constants are smaller than the coupling constant corresponding to interactions of smooth components of the density, and the in-chain interactions are larger (or much larger) than the interchain interactions,

$$g_{2k_F}^\perp \lesssim g_0^\perp < g_{2k_F} \lesssim J_{2k_F} \sim g_4 \ll v_F. \quad (15)$$

The smallness of the transverse couplings as compared to the in-chain coupling constants assures that at high energy the system may be viewed as a collection of weakly perturbed 1D conductors. The smallness of all coupling constants as compared to v_F indicates that weak-coupling arguments may be applied.

B. Effective description

It is tempting to study the low-temperature phase diagram of H [Eq. (1)] with the help of the mean-field approximation.

Yet, one has to keep in mind that this idea is wrong. It is demonstrated by Prigodin and Firsov,²⁶ who investigated the renormalization-group (RG) flow of the Q1D metal, that at high energy the Cooper channel and the particle-hole channel are coupled, the usual ladder summation is not adequate, and it is necessary to use the parquet approximation. Failure of the ladder approximation implies the failure of the mean-field theory since the two approaches are equivalent.

Fortunately, this coupling between the channels is a 1D feature, which disappears at sufficiently low energy. Indeed, it is also proven in Ref. 26 that the weakly interacting Q1D Fermi system experiences the dimensional crossover at low energy; below the crossover the channels decouple, and the ladder approximation (hence, the mean-field theory) is valid again.

Thus, if we need to know low-energy properties of the model (e.g., the phase diagram), it is enough to derive the effective Hamiltonian valid below the dimensional crossover for this Hamiltonian may be analyzed with the help of usual mean-field approximation.

How does this Hamiltonian look like? This question is addressed in several theoretical papers.¹⁻⁴ These papers discuss in detail the dependence of the effective coupling constants on the bare one. However, for our purposes it is enough to guess general features of the low-energy Hamiltonian. Our conjecture is based on two assumptions about RG flow: (i) at high energy the transverse single-electron hopping is the most relevant operator in the problem and the crossover occurs when the effective transverse hopping becomes comparable to the running cutoff; (ii) at high energy the SDW and CDW susceptibilities are dominant; among these two the SDW susceptibility prevails.

What do these statements mean physically? Assumption (i) is valid provided that bare interactions are sufficiently weak (for an accurate criterion of the single-electron hopping relevance one can consult, e.g., Ref. 27). It guarantees that our low-energy model is Fermi liquid with weak effective coupling constants and low effective anisotropy,

$$\tilde{r} = \tilde{t}/\tilde{v}_F \tilde{\Lambda} \sim 1. \quad (16)$$

When (i) is violated, the system freezes into an ordered state (typically, SDW or CDW) before reaching the Fermi-liquid regime. Needless to say, our analysis is inapplicable in such a situation.

Assumption (ii) is a consequence of the electron repulsion combined with the fact that high-energy physics is purely one dimensional. It is known that the 1D metal has strongly divergent susceptibilities toward SDW and CDW. Of these two, the former is stronger due to the in-chain backscattering g_1 . Because of all this, the SDW susceptibility prevails in the high-energy regime.

This effect has nothing to do with the nesting properties of the actual Fermi surface, which is a low-energy feature. Moreover, one can say that this abundance of the high-energy modes, enhancing SDW correlations regardless of the nesting, is a peculiarity of Q1D metal, which makes its physics so unusual. Taking (i) and (ii) into account we can write the following effective Hamiltonian:

$$\tilde{H} = \sum_i \tilde{H}_i^{\text{kin}} + \tilde{H}_i^{\text{pp}} + \sum_{ij} \tilde{H}_{ij}^{\text{hop}} + \tilde{H}_{ij}^{\text{pp}} + \tilde{H}_{ij}^{\text{SS}}. \quad (17)$$

The spin-spin transverse interaction term $\tilde{H}_{ij}^{\text{SS}}$ is equal to

$$\tilde{H}_{ij}^{\text{SS}} = \int dx [\tilde{J}_0^\perp (i-j) \mathbf{S}_i \cdot \mathbf{S}_j + \tilde{J}_{2k_F}^\perp (i-j) (\mathbf{S}_{2k_F i} \cdot \mathbf{S}_{-2k_F j} + \text{H.c.})], \quad (18)$$

$$\mathbf{S} = \sum_{\rho\sigma\sigma'} \tilde{\tau}_{\sigma\sigma'} \psi_{\rho\sigma}^\dagger \psi_{\rho\sigma'}. \quad (19)$$

This term, although absent in the microscopic Hamiltonian, appears at low energies. Other terms of Eq. (17), \tilde{H}_i^{kin} , \tilde{H}_i^{pp} , $\tilde{H}_{ij}^{\text{hop}}$, and $\tilde{H}_{ij}^{\text{pp}}$, have the same structure as the corresponding operators without tilde (H_i^{kin} , H_i^{pp} , H_{ij}^{hop} , and H_{ij}^{pp}) but the former has renormalized constants (\tilde{v}_F instead of v_F , \tilde{t} instead of t , and \tilde{g} 's instead of g 's). On top of this, the cutoff of the effective theory is much smaller than the microscopic cutoff: $\tilde{\Lambda} \ll \Lambda$.

Hierarchy of the effective coupling constants differs from Eqs. (14) and (15). At the dimensional crossover the transverse hopping becomes comparable to the cutoff [see Eq. (16)]. The effective system remains anisotropic (for example, its Fermi surface consists of two warped sheets disconnected from each other), yet, this anisotropy is not as strong as the anisotropy of the original microscopic system.

Since at high energy the dominating fluctuations are SDW and CDW, $2k_F$ coupling constants are enhanced,

$$\tilde{g}_{2k_F} \gg \tilde{g}_4, \quad (20)$$

$$\tilde{J}_{2k_F} \gg \tilde{g}_4, \quad (21)$$

$$\tilde{J}_{2k_F}^\perp \gg \tilde{J}_0^\perp, \quad (22)$$

$$\tilde{g}_{2k_F}^\perp \gg \tilde{g}_0^\perp. \quad (23)$$

All coupling constants are smaller than the renormalized Fermi velocity \tilde{v}_F . It is tempting to declare that since SDW correlations dominate over CDW correlations in the high-energy regime, the SDW coupling constant $\tilde{J}_{2k_F}^\perp$ is bigger than the CDW constant $\tilde{g}_{2k_F}^\perp$. However, this is not necessarily true for bare $J_{2k_F}^\perp$ is zero while $g_{2k_F}^\perp \neq 0$. This might affect the outcome at the crossover scale.

III. PHASE DIAGRAM

In this section we apply the mean-field analysis to the effective Hamiltonian \tilde{H} [Eq. (17)].

A. Density-wave phases

The low-temperature phase of the effective Hamiltonian depends on the nesting properties of the Fermi surface. Assume first that only nearest-neighbor hopping amplitude t_1 is

nonzero. In this case the Fermi surface nests perfectly. The SDW susceptibility is equal to

$$\chi_{\text{SDW}} = \frac{1}{\pi\tilde{v}_F} \ln \left(\frac{2\tilde{v}_F\tilde{\Lambda}}{T} \right). \quad (24)$$

The CDW susceptibility is the same. As it is obvious from Eq. (18), the coupling constant for SDW is equal to $\tilde{g}_{\text{SDW}} = \tilde{J}_{2k_F} + z\tilde{J}_{2k_F}^\perp$, where z is the number of the nearest neighbours. The usual mean-field equation for the critical temperature $\tilde{g}_{\text{SDW}}\chi_{\text{SDW}}(T_{\text{SDW}}) = 1$ gives us the formula for T_{SDW} ,

$$T_{\text{SDW}}^{\text{max}} = 2\tilde{v}_F\tilde{\Lambda} \exp[-\pi\tilde{v}_F/(\tilde{J}_{2k_F} + z\tilde{J}_{2k_F}^\perp)]. \quad (25)$$

The superscript ‘‘max’’ is to remind us that at perfect nesting the transition temperature is the highest. The CDW coupling constant $\tilde{g}_{\text{CDW}} = \tilde{g}_{2k_F} + z\tilde{g}_{2k_F}^\perp$ may be larger or smaller than \tilde{g}_{SDW} depending on the bare values of g , g^\perp , and J_{2k_F} . The density-wave type is determined by comparison of the coupling constants. Namely, if it is true that

$$\tilde{g}_{\text{CDW}} = \tilde{g}_{2k_F} + z\tilde{g}_{2k_F}^\perp > \tilde{g}_{\text{SDW}} = \tilde{J}_{2k_F} + z\tilde{J}_{2k_F}^\perp, \quad (26)$$

the ground state is CDW; otherwise, it is SDW. When the nesting is spoiled (for example, by introducing next-to-nearest-neighbor hopping amplitude t_2), the density-wave critical temperature decreases. This happens because antineesting destroys the divergence of the susceptibility. For example, one might write for SDW (the case of CDW is identical),

$$\chi_{\text{SDW}} \propto \frac{1}{\pi\tilde{v}_F} \begin{cases} \ln(2\tilde{v}_F\tilde{\Lambda}/T), & \text{if } T > \tilde{t}_2, \\ \ln(2\tilde{v}_F\tilde{\Lambda}/\tilde{t}_2), & \text{if } T < \tilde{t}_2, \end{cases} \quad (27)$$

where \tilde{t}_2 is the renormalized value of t_2 . When \tilde{t}_2 is bigger than certain critical value,

$$\tilde{t}_2 > t_2^c = T_{\text{SDW}}^{\text{max}}, \quad (28)$$

the mean-field equation $\tilde{g}_{\text{SDW}}\chi_{\text{SDW}}(T_{\text{SDW}}) = 1$ has no solution. Thus, exponentially small \tilde{t}_2 is enough to destroy the density-wave phase.

B. Superconductivity

When the antineesting destroys the density wave, the system becomes superconducting. To demonstrate this let us introduce the following set of Cooper-pair-creation operators,

$$(\hat{\Delta}_{ij})_{\sigma\sigma'} = \psi_{L\sigma i}^\dagger \psi_{R\sigma' j}^\dagger. \quad (29)$$

Operator $(\hat{\Delta}_{ij})_{\sigma\sigma'}$ creates a Cooper pair composed of a left-moving electron of spin σ on chain i and of a right-moving electron of spin σ' on chain j . Matrix $\hat{\Delta}_{ij}$ may be symmetrized with respect to the chain indices,

$$\hat{\Delta}_{ij}^{s/a} = \frac{1}{2}(\hat{\Delta}_{ij} \pm \hat{\Delta}_{ji}). \quad (30)$$

The superscript ‘‘s’’ (‘‘a’’) stands for ‘‘symmetric’’ (‘‘antisymmetric’’). Further, it is convenient to write $\hat{\Delta}_{ij}^{s/a}$ as a sum of

three symmetric matrices $i\tilde{\tau}^\nu$ and one antisymmetric matrix $i\tilde{\tau}^\nu$,

$$\hat{\Delta}_{ij}^{s/a} = \frac{1}{\sqrt{2}} [\mathbf{d}_{ij}^{s/a} \cdot (i\tilde{\tau}^\nu) + \Delta_{ij}^{s/a} i\tilde{\tau}^\nu], \quad (31)$$

where $\tilde{\tau} = (\tilde{\tau}^x, \tilde{\tau}^y, \tilde{\tau}^z)$ is a vector composed of three Pauli matrices. Operator $\Delta_{ij}^{s/a} (\mathbf{d}_{ij}^{s/a})$ creates a Cooper pair in a singlet (triplet) state. Using these operators we can rewrite \tilde{H}_{ij}^{pp} and \tilde{H}_{ij}^{SS} as

$$\sum_{ij} \tilde{H}_{ij}^{pp} + \tilde{H}_{ij}^{SS} = - \sum_{ij} \int dx [\tilde{g}_{x^2-y^2} \Delta_{ij}^s (\Delta_{ij}^s)^\dagger + \tilde{g}_{xy} \Delta_{ij}^a (\Delta_{ij}^a)^\dagger + \tilde{g}_f \mathbf{d}_{ij}^s \cdot (\mathbf{d}_{ij}^s)^\dagger + \tilde{g}'_f \mathbf{d}_{ij}^a \cdot (\mathbf{d}_{ij}^a)^\dagger] + \dots, \quad (32)$$

where the ellipsis stands for the terms, which cannot be expressed as a product of a Cooper-pair creation and Cooper-pair destruction operators (for example, $\psi_{L\sigma}^\dagger \psi_{L\sigma'} \psi_{L\sigma''}^\dagger \psi_{L\sigma''}$). The coupling constants are

$$\tilde{g}_{x^2-y^2} = 6\tilde{J}_{2k_F}^\perp - 2\tilde{g}_{2k_F}^\perp + 6\tilde{J}_0^\perp - 2\tilde{g}_0^\perp, \quad (33)$$

$$\tilde{g}_{xy} = -6\tilde{J}_{2k_F}^\perp + 2\tilde{g}_{2k_F}^\perp + 6\tilde{J}_0^\perp - 2\tilde{g}_0^\perp, \quad (34)$$

$$\tilde{g}_f = 2\tilde{J}_{2k_F}^\perp + 2\tilde{g}_{2k_F}^\perp - 2\tilde{J}_0^\perp - 2\tilde{g}_0^\perp, \quad (35)$$

$$\tilde{g}'_f = -2\tilde{J}_{2k_F}^\perp - 2\tilde{g}_{2k_F}^\perp - 2\tilde{J}_0^\perp - 2\tilde{g}_0^\perp. \quad (36)$$

We see from Eq. (36) that the order parameter $\langle \mathbf{d}^a \rangle$ is always zero since the coupling constant \tilde{g}'_f is always negative.

Three other order parameters may be nonzero. Consider first $d_{x^2-y^2}$ -wave ($\langle \Delta^s \rangle \neq 0$). This type of superconductivity is at least metastable if

$$\tilde{g}_{x^2-y^2} > 0 \Leftrightarrow 3\tilde{J}_{2k_F}^\perp > \tilde{g}_{2k_F}^\perp. \quad (37)$$

In the latter inequality we neglected \tilde{g}_0^\perp and \tilde{J}_0^\perp for they are small [see Eqs. (22) and (23)].

Triplet f -wave superconductivity ($\langle \mathbf{d}^s \rangle \neq 0$) is always metastable since $\tilde{g}_f > 0$ [provided that Eqs. (22) and (23) are satisfied]. This guarantees that after the density wave is destroyed by the antineesting, the Q1D metal becomes a superconductor.

Singlet d_{xy} -wave superconductivity ($\langle \Delta^a \rangle \neq 0$) is metastable if $\tilde{g}_{xy} > 0$, which is equivalent to

$$\tilde{g}_{2k_F}^\perp > 3\tilde{J}_{2k_F}^\perp. \quad (38)$$

The true ground state is determined by comparison of the mean-field transition temperatures for different superconducting order parameters. These temperatures are the solutions of the equations $g_\alpha \chi_\alpha(T_c^\alpha) = 1$, where α is either f , or $d_{x^2-y^2}$, or d_{xy} .

Let us compare first $T_c^{x^2-y^2}$ and T_c^f . These two order parameters have identical orbital structures. Therefore, their susceptibilities are the same: $\chi_{x^2-y^2} = \chi_f$. Consequently, in order

to determine the relative stability of $d_{x^2-y^2}$ -wave and f -wave we must compare $\tilde{g}_{x^2-y^2}$ and \tilde{g}_f . Specifically, $T_c^{x^2-y^2} > T_c^f$ if

$$\tilde{g}_{2k_F}^\perp < \tilde{J}_{2k_F}^\perp. \quad (39)$$

Equation (39) implies that spin-density fluctuations, which enhance $\tilde{J}_{2k_F}^\perp$, favor $d_{x^2-y^2}$ -wave over f -wave.^{5,15} Thus, proximity to the SDW phase promotes the former type of order. On the contrary, close to CDW the charge-density fluctuations intensify, as a result of which effective coupling $\tilde{g}_{2k_F}^\perp$ grows, advancing the f -wave superconductivity.

To make this argument more concrete, consider the transition separating CDW and superconductivity. Stability of CDW implies that Eq. (26) is fulfilled. This inequality may be rewritten as

$$\tilde{g}_{2k_F} - \tilde{J}_{2k_F} > \frac{z}{4} (\tilde{g}_{x^2-y^2} - \tilde{g}_f). \quad (40)$$

Observe that the bare constants satisfy [see Eqs. (9) and (10)]

$$g_{2k_F} < J_{2k_F}. \quad (41)$$

If we assume that the renormalized coupling constants \tilde{g}_{2k_F} and \tilde{J}_{2k_F} satisfy the same inequality,

$$\tilde{g}_{2k_F} < \tilde{J}_{2k_F}, \quad (42)$$

then we obtain

$$\tilde{g}_{x^2-y^2} - \tilde{g}_f < 0. \quad (43)$$

This means that CDW cannot have common boundary with $d_{x^2-y^2}$ -wave superconductivity.

However, inequality Eq. (41) is not equivalent to Eq. (42). The former could be violated but the latter cannot. Therefore, this argumentation points to a trend rather than establishes a hard connection between the density-wave type and the order-parameter symmetry.

The coupling constant for d_{xy} -wave is always smaller than \tilde{g}_f ,

$$\tilde{g}_f - \tilde{g}_{xy} = 8\tilde{J}_{2k_F}^\perp > 0. \quad (44)$$

This does not necessarily mean that f -wave superconductivity always overshadows the d_{xy} -wave superconductivity. These two have different orbital structures (the former is symmetric with respect to inversion of the transverse coordinates while the latter is antisymmetric). Thus, it is possible to choose the density of states in such a way that $\chi_{xy} > \chi_f$. If this happens and if the difference between \tilde{g}_f and \tilde{g}_{xy} [see Eq. (44)] is not too large, the d_{xy} -wave order parameter may be more stable than f -wave. Therefore, we conclude that, when $d_{x^2-y^2}$ -wave is unstable, both f -wave and d_{xy} -wave can be possible choices for the symmetry of the order parameter.

It is also important to note that the superconductivity becomes possible only in a system with sufficiently pronounced anisotropy ($r \ll 1$). Otherwise, the 1D renormalization is weak and

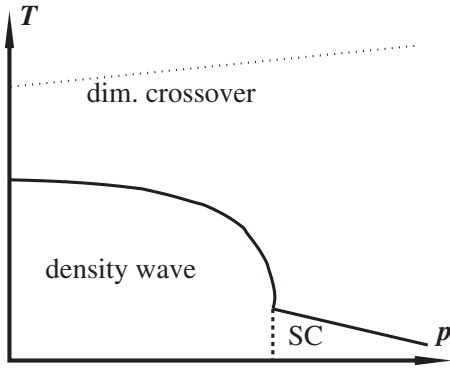


FIG. 1. Qualitative phase diagram of our model on the plane pressure-temperature. Growth of the external pressure acts to increase the transverse hopping, which decreases the anisotropy and increases the antinesting. Solid lines show second-order phase transitions into the density-wave state (SDW or CDW) and the superconducting phase. Dashed line shows the first-order transition between the density wave and the superconductivity. The dotted line at high temperature marks location of the dimensional crossover.

$$\tilde{g}_{2k_F}^\perp \approx g_{2k_F}^\perp, \quad \tilde{g}_0^\perp \approx g_0^\perp, \quad \tilde{J}_{0,2k_F}^\perp \approx 0. \quad (45)$$

As a result, instead of Eqs. (22) and (23), one has to use Eq. (15). In this case all superconducting coupling constants are negative because they are dominated by $-2\tilde{g}_0^\perp$ term.

In Fig. 1 we present the phase diagram, which emerges from our discussion. It is drawn on the pressure-temperature plane. The effect of the pressure is twofold. First, it increases the transverse hopping, which leads to increase in the anisotropy ratio r . As a result, the dimensional crossover temperature grows and the superconducting critical temperature decreases.

Second, the pressure increases the next-to-nearest-neighbor hopping, spoiling the nesting properties of the Fermi surface. Thus, the density-wave transition temperature vanishes when the pressure exceeds some critical value p_c . This explains the major features of our phase diagram.

IV. DISCUSSION

We demonstrated under rather general assumptions that (i) Q1D metal has a superconducting ground state and (ii) the symmetry of the order parameter is sensitive to the details of the interaction and the density of states.

This implies that the “universal” phase diagram of the Bechgaard salts²⁵ is a robust feature of Q1D metals, easily reproducible theoretically. At the same time, prediction of the order-parameter symmetry on the basis of the microscopic model is virtually impossible for it requires very accurate calculations of the competing states’ energies.

One must remember that different Q1D organic superconductors, despite many similarities they share, may have different symmetry of the superconducting order parameter. Furthermore, it is possible that an individual sample experiences a phase transition between different types of superconductivity if the external parameters (pressure, magnetic field) change. It is possible that such a phenomena is indeed observed experimentally; within the superconducting region of (TMTSF)ClO a phase transition is detected when the external magnetic field exceeds some critical value.²⁴

Our approach, however, has some limitations. Namely, it is not applicable in situations, where the dimensional crossover occurs due to transverse interaction rather than transverse hopping.²⁸

To conclude we discussed the symmetry of the order parameter in Q1D metallic Fermi system. It is demonstrated that for a certain class of Q1D superconductors the order-parameter symmetry is a nonuniversal feature. It is determined by a delicate interplay of microscopic constants characterizing the system. The order-parameter type may easily change in response to variation in external (pressure) or internal (doping) factors.

ACKNOWLEDGMENT

The author is grateful for the support provided by the FRBR under Grants No. 08-02-00212 and No. 09-02-00248.

¹B. Guay and C. Bourbonnais, *Synth. Met.* **103**, 2180 (1999).
²C. Bourbonnais and L. G. Caron, *Europhys. Lett.* **5**, 209 (1988).
³A. V. Rozhkov, *Phys. Rev. B* **68**, 115108 (2003).
⁴A. V. Rozhkov, arXiv:0708.1884 (unpublished).
⁵J. C. Nickel, R. Duprat, C. Bourbonnais, and N. Dupuis, *Phys. Rev. B* **73**, 165126 (2006).
⁶R. Duprat, C. Bourbonnais, *Eur. Phys. J. B* **21**, 219 (2001).
⁷J. C. Nickel, R. Duprat, C. Bourbonnais, and N. Dupuis, *Phys. Rev. Lett.*, **95**, 247001 (2005).
⁸N. Dupuis, C. Bourbonnais, and J. C. Nickel, *Low Temp. Phys.* **32**, 380 (2006).
⁹C. Bourbonnais, arXiv:cond-mat/0204345 (unpublished).
¹⁰T. Aonuma, Y. Fuseya, and M. Ogata, *J. Phys. Soc. Jpn.* **78**, 034722 (2009).
¹¹K. Kuroki, *J. Phys. Soc. Jpn.* **75**, 051013 (2006).
¹²Y. Fuseya and Y. Suzumura, *J. Phys. Soc. Jpn.* **74**, 1263 (2005).

¹³Y. Tanaka and K. Kuroki, *Phys. Rev. B*, **70**, 060502(R) (2004).
¹⁴Kazuhiko Kuroki and Yukio Tanaka, *J. Phys. Soc. Jpn.* **74**, 1694 (2005).
¹⁵K. Kuroki, R. Arita, and H. Aoki, *Phys. Rev. B* **63**, 094509 (2001).
¹⁶N. Belmechri, G. Abramovici, M. Heritier, S. Haddad, and S. Charfi-Kaddour, *EPL* **80**, 37004 (2007).
¹⁷N. Belmechri, G. Abramovici, and M. Heritier, *EPL* **82**, 47009 (2008).
¹⁸I. J. Lee, S. E. Brown, W. G. Clark, M. J. Strouse, M. J. Naughton, W. Kang, and P. M. Chaikin, *Phys. Rev. Lett.* **88**, 017004 (2001).
¹⁹I. J. Lee, D. S. Chow, W. G. Clark, M. J. Strouse, M. J. Naughton, P. M. Chaikin, and S. E. Brown, *Phys. Rev. B* **68**, 092510 (2003).
²⁰N. Joo, P. Auban-Senzier, C. R. Pasquier, P. Monod, D. Jérôme,

- and K. Bechgaard, Eur. Phys. J. B **40**, 43 (2004).
- ²¹I. J. Lee, M. J. Naughton, G. M. Danner, and P. M. Chaikin, Phys. Rev. Lett. **78**, 3555 (1997).
- ²²J. I. Oh and M. J. Naughton, Phys. Rev. Lett. **92**, 067001 (2004).
- ²³Stéphane Belin and Kamran Behnia, Phys. Rev. Lett. **79**, 2125 (1997).
- ²⁴J. Shinagawa, Y. Kurosaki, F. Zhang, C. Parker, S. E. Brown, D. Jerome, K. Bechgaard, and J. B. Christensen, Phys. Rev. Lett. **98**, 147002 (2007).
- ²⁵H. Wilhelm, D. Jaccard, R. Duprat, C. Bourbonnais, D. Jerome, J. Moser, C. Carcel, and J. M. Fabre, Eur. Phys. J. B **21**, 175 (2001).
- ²⁶V. N. Prigodin and Yu. A. Firsov, Sov. Phys. JETP **49**, 369 (1979).
- ²⁷A. O. Gogolin, A. A. Nersesyan, and A. M. Tsvelik, *Bosonization and Strongly Correlated Systems* (Cambridge University Press, Cambridge, England, 1998).
- ²⁸L. Caron and C. Bourbonnais, Physica B & C **143B**, 453 (1986).